Curricular Unit of Biomechanics of Motion
2019/20, Instituto Superior Técnico, Lisboa, Portugal

DYNAMIC ANALYSIS OF HUMAN MOVEMENT: GAIT AND STANDING LONG JUMP

André Vieira (83812)[1], Jeanne Evrard (95177)[2], Manuel Madeira (83836)[3] and Maria Parreira (83844)[4]

[1]*Instituto Superior Técnico,*
Integrated Master's in Biomedical Engineering
andre.s.vieira@tecnico.ulisboa.pt

[2] *Université Catholique de Louvain,*
Integrated Master's in Mechanical Engineering
jeanne.evrard@student.uclouvain.be

[3]*Instituto Superior Técnico,*
Integrated Master's in Biomedical Engineering
manuel.madeira@tecnico.ulisboa.pt

[4] *Instituto Superior Técnico,*
Integrated Master's in Biomedical Engineering
maria.parreira@tecnico.ulisboa.pt

ABSTRACT - *Similarly to kinematic analysis, dynamic analysis of motion is an extremely useful tool to evaluate the performance of a certain movement, whether in the context of sports or identification of injuries. In the present work, a dynamic analysis was performed to study the gait cycle and a standing long jump (SLJ) in a multibody biomechanical system. The data was acquired in the Biomechanics of Motion Lab at Instituto Superior Técnico and the 2D Multibody Model was defined with MATLAB. Complementary electromyography (EMG) activity was also obtained and analyzed. For both movements the ground reaction forces, joint moment and joint power were analyzed, with the results being consistent with the ones observed in the literature. For the SLJ, however, the comparison of results was limited due to the lack of previous studies. As for the gait cycle, the results showed that this consisted of a slow cadence movement, confirming the conjecture of the previous work. Overall, this mathematical model proved to be an important tool to tackle the problem at hands, with consistent results and allowing for a reliable analysis of motion.*

1 Introduction

Dynamics is the field of classical mechanics that is concerned with the study of forces involved in the performance of a movement and is of particular importance in the field of biomechanics, as researchers continuously seek to improve computational models to perform human motion analysis. These multibody models requires the use of formulations to describe their dynamic equilibrium conditions, such as those based on Cartesian coordinates, natural coordinates, joint coordinates or Kane's formalism.[1]

Dynamic analysis can be of two types, depending on its main objective. Forward dynamic analysis can be used when the goal is to enhance performance, i.e., to find the best motion to perform a certain task. On the other hand, an inverse dynamic analysis is useful when the motion is completely known, and one pretends to find the internal forces responsible for its execution.[1] The present work consists of the forward dynamic analysis of a gait cycle and standing long jump, of a multibody system using Cartesian coordinates.

Note that this report takes into consideration what was mentioned in the previous part of this same project[2] thus only new steps and results are presented. Appendices are used for extra information and some clarification, in order to focus more on the results and discussion, the main pedagogical components of this project.

2 Methodology

2.1 Data acquisition

The acquisition of the data used was the same as was described in part I.[2] Additionally, muscle activity was acquired with four electromyography (EMG) electrodes, placed in the subject's Gastrocnemius Medialis, Tibialis Anterior, Rectus Femoris and Biceps Femoris muscles, was also considered for the dynamic analysis. The three components of the external forces (ground reactions) were also collected along three force plates placed below the subject's path, allowing for the estimation of the center of pressure in each moment of each movement.

2.2 Preprocessing

Once the raw data are obtained, preprocessing is called for. Figure 2.1 references the functions implemented in MATLAB for the preprocessing part. Some of the functions represented were already described in the kinematic analysis of these movements,[2] so their descriptions are omitted here but can be accessed in Appendix A.

ReadDraftInput() will adapt the previously built draft model and consider the ground reactions forces collected and store the mass ratio and radius of gyration ratio (data can be consulted in Appendix B. These values were then used in the *ComputeBodyProperties()* function to estimate and store the mass and inertia values of each body. Mass is estimated by multiplying the total body mass by the previously stored mass ratio, while the inertia can be expressed as follows: $J = MR^2$, with M being the mass of the limb and R the radius of gyration.

ReadGRF() is used to process the force plate data, with a sampling frequency of 100Hz. Forces are collected and filtered with a low-pass Butterworth and using Residual Analysis to find the

optimal cut-off frequency, whereas Centers of Pressure (CoPs) are filtered with a fixed frequency of 10Hz.

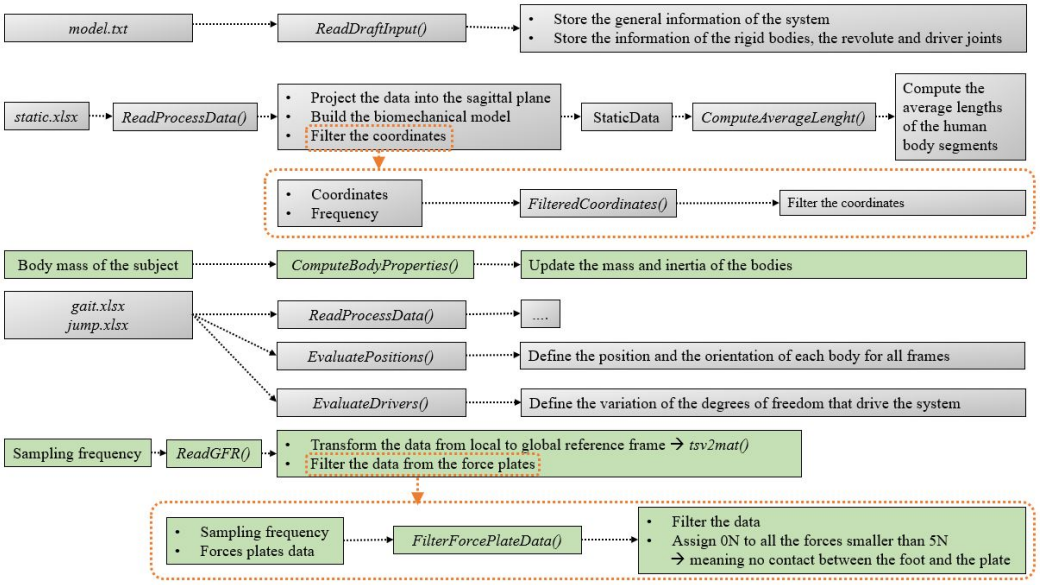

Figure 2.1: Functions implemented in the preprocessing part. Green boxes represent new steps absent in the kinematics analysis

On the note of filtration, Appendix C displays the cutoff frequencies for each of the bodies, obtained via the function *FilteredCoordinates* -used for part I as well - which applies residual analysis. It is interesting to analyse how bodies associated with different parts of a movement display different optimal cutoff frequencies.

Finally, *WritesModelInput()* will compute a summary of the data and variables created, similarly to what was done before. Data from force plates was kept with a precision of 20 digits.

2.3 Processing

The relation between forces and motion of a system are described by the **equations of motion**. To obtain these equations for a general multibody system, the principle of *Virtual Power* can be applied:

$$P^* = \dot{q}^{*T}(M\ddot{q} - g_{ext}) \tag{2.1}$$

where $\dot{q}^*$ is a vector of virtual velocities,M is a matrix with the overall mass of the system, $\ddot{q}$ is a vector of generalized accelerations and g_{ext} corresponds to the external forces. $M\ddot{q}$ represents the inertial forces of the system. This system does not take into account the internal forces $g_{int}$and, to introduce them the *Lagrange multipliers method* is applied, with the internal forces being calculated as $g_{int} = \Phi_q^T\lambda$, with λ the vector of the lagrange multipliers. This way, according to D'Alembert principle for dynamic equilibrium,[3] the virtual power of a multibody system is equal to zero and the following condition is obtained:

$$P^* = \dot{q}^{*T}(M\ddot{q} + \Phi_q^T\lambda - g_{ext}) = 0 \tag{2.2}$$

To make it a fully solvable system with one unique solution, the acceleration kinematic constraint equations are needed: $\Phi_q \ddot{q} = \gamma$. Hence, the final set of equations computed to solve the dynamic analysis of a multibody system are expressed as follows:

$$\begin{bmatrix} M & \Phi_q^T \\ \Phi_q & 0 \end{bmatrix} \begin{Bmatrix} \ddot{q} \\ \lambda \end{Bmatrix} = \begin{Bmatrix} g \\ \gamma \end{Bmatrix} \tag{2.3}$$

The problem is then solved through an iterative process, starting from a set of initial conditions. See Appendix D) for this and more detail on equations used for the processing part.

Baumgarte stabilizer is implemented with feedback parameters α and β a value of 5.The function that implements external forces is called *BuildForceVector()* and mass matrices are calculated through *BuldMassMatrix()*.

Newton-Raphson method is again applied, with two stopping criteria: maximum error of 10^{-6} or maximum number of iterations 12 (although solution was generally found after a maximum of 3 iterations).

It is important to note that, for the second motion (SLJ), since both feet were stepping on the same plate, thus impairing the precision of the results, which were by default applied on one foot. In order to overcome this fact, we considered the magnitude of the force in each axis to be uniformly divided between the two bodies (two feet) and their moment was calculated and applied to the g vector separately (function *GroundReactionSJL* calculates the forces and *ApplyForce* sums them to the g vector).

As a final note, due to the fact that a spline interpolation of 3^{rd} order is being used to turn our data into a C^2 smooth function, we are enforcing the second derivative of the drivers' data to be approximated by linear piecewise approximations (1^{st} order splines), ending up on the introduction of significant noise on this component of our analysis. For the 1^{st} derivative a smaller but still similar behaviour was observed - a problem that had been noted in the first part of the project. Given this, a smoothing of both derivatives were carried out in order to enhance our results, resorting to residual analysis with a minimum correlation of 0.95.

3 Results

3.1 Gait - Dynamic Analysis

The previous analysis[2] allowed for the conclusion that the motion at hands is a slow walk rather than normal gait, mostly due to the fact that the subject was trying to step on the force sensor plates placed below their path - thus possibly impairing the data collected, as the steps would have a bigger length and duration due to the effort of hitting certain targets on the ground.

An important step to note for the results introduced below is the normalization performed, for both the variable under study (which is divided by body weight) and cadence (displayed as a percentage of the stride), allowing for the analysis of the results obtained in contrast with those across literature. It is also important to point out that the analysis will focus on the lower limbs, as this is more telling of the overall gait motion and, in fact, can be a great tool for the assessment of the physiological condition of an individual. the subject and precision on the results, as a form of diagnosis.

Ground Reaction Forces

The ground reaction forces (GRFs) as measured by the platforms reflect the net vertical and shear forces acting on the surface of the platform - they are the algebraic summation of the mass-acceleration products of all body segments while the foot is in contact with the platform. Figure 3.1 displays the results for each of the plates and compares them wit the literature.

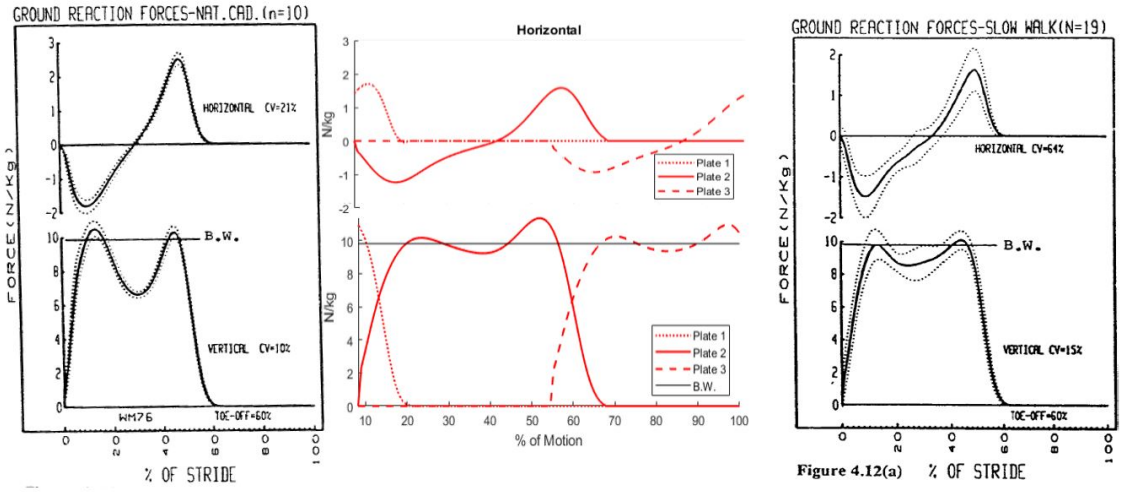

Figure 3.1: Ground Reaction Forces, horizontal (top) and vertical (bottom) (N/kg). B.W. - Bodyweight/kg. Left: Natural cadence, retrieved from *Winter(1987)*.[4] Center: obtained from lab data, after processing, and representing the GRFs of each of the plates. Right: Slow cadence, retrieved from *Winter(1987)*.[4]

Note how, consistently with findings in the previous work, the GRFs obtained from lab data seem more closely related to those belonging to a slow cadence. In fact, one can correlate the peaks of the GRFs and velocity of walking[5] - for instance, as velocity decreases, the amplitude of the peaks (maxima and minimum) are expected to decrease as well. These peaks can be interpreted physically: horizontal forces have an initial negative phase - reflecting the net slowdown of the body - and a positive phase which represents its acceleration; the M-shaped vertical force, on the other hand, has its first peak representing an upwards acceleration of the center of gravity during early stance, whereas the second peak corresponds to a deceleration at the end of the stance.

The amplitude of the peaks (absolute maximum to minimum) is of 2.1199 N/kg, higher than what is expected for a slow gait (1.5 N/kg)[4] and instead closer that the normal gait (2 N/kg), with an overall mean value of 8.2763 N/kg which is close to the values in literature.

Moments of Force

Moments of force are the net result of forces from muscles and ligaments as well as friction (although, for gait, these are minimal as the angles of joints don't reach their extremes - making the moments a result of the muscular activity only .

The moments of force with respect to the right hip joint, right knee joint and right ankle joint are presented below (Figure3.2), where knee extension, hip extension and plantar flexion are considered positives.

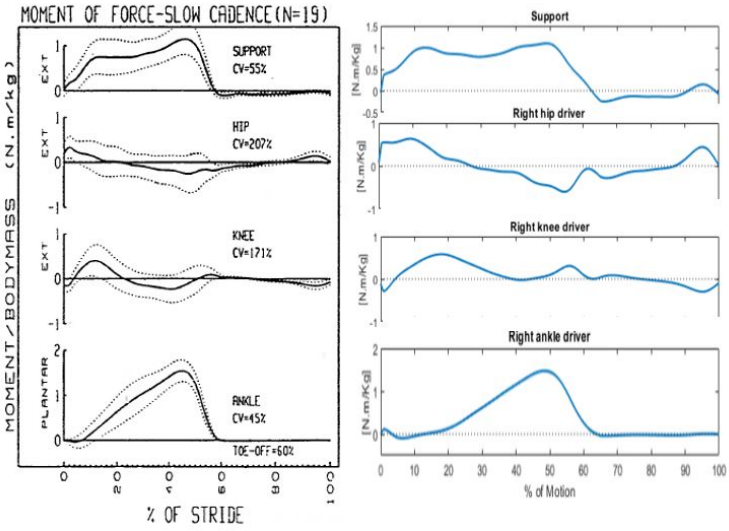

Figure 3.2: Support moment and moments of force on right hip, right knee and right ankle joints during gait (N.m/kg).Left: Retrieved from *Winter(1987)*.[4] Right: results obtained from lab data, after processing.

The support moment reflects a pattern set by the lower limbs during stance. It is described by Winter(1987) and is calculated as:

$$M_s = M_h + M_k + M_a \tag{3.1}$$

where h, k, a refer to the moments of the hip, knee and ankle, respectively. Because the motion of each of the first two joints is highly correlated, the support moment is expected to remain the same throughout trials. As for the moments of force, note that they are compared to those referring to a slow cadence and are remarkably similar, with some oscillations possibly attributed to hesitation of the subject upon stepping on the force plates.

Joint Power

The mechanical power of a joint reflects the eccentric and concentric phases of muscles as they recruit the mechanical energy necessary to accomplish movement, and can be calculated as such:

$$P_j = M_j.w_j \tag{3.2}$$

When power is positive, muscles are generating energy (concentric contraction); when negative, it implies absorption (eccentric contraction).

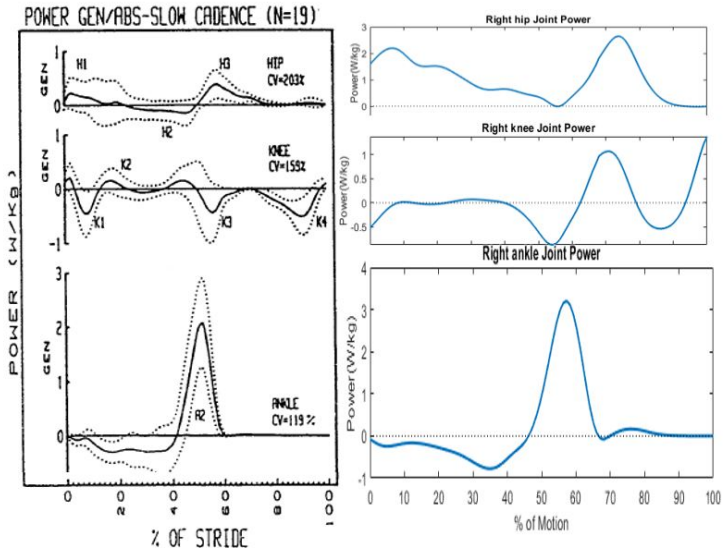

Figure 3.3: Joint Power of right hip, right knee and right ankle joints during gait(W/kg).Left: Retrieved from *Winter(1987)*.[4] Right: results obtained from lab data, after processing.

Initially, the hip is expected to generate energy due to concentric muscle contraction,[6] followed by energy absorption until pre-swing, with yet another peak of energy absorption. The knee will mostly absorb energy during swing, which will be used in the initial contact. As for the ankle, the peak is representative of the moment the foot pushes the ground and projects the individual forwards, hence a peak energy generated, after which the only force applied on each segment is its weight thus making the power exchange negligible. The results obtained are quite similar to those expected when considering standard deviations.
.[6]

Related to this point, a final note is that any regular, repeated motion will have a pattern which is characteristic of each subject under study - inter-subject variability is the reason why large databases of biomechanical motion data are of the upmost importance to establish a transverse pattern - but one must also consider intra-subject variability inherent to our physical, as well as psychological status. With all of these variants, it is indeed impressive how the gait can be used as a form of diagnosis.

3.2 Standing Long Jump - Dynamic Analysis

Ground Reaction Forces

As previously mentioned, the GRFs represent the forces exerted on the plates through the analyzed motion. In the case studied, the vertical (F_y) and horizontal (F_x) components (along the sagital plane) were studied, being depicted in Fig.3.4

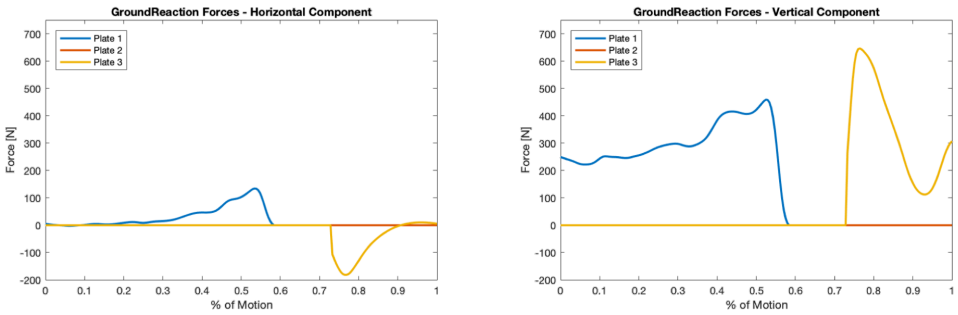

Figure 3.4: GRFs for each foot obtained for the lab data available. The horizontal (left) and vertical (right) component are represented for the 3 plates (1, 2 and 3), which were numbered accordingly to the motion direction.

Through observation of Fig.3.4, it should be mentioned that even though a quick look might induce one to think that the horizontal component is almost negligible, that is not true. In fact, our subject has a mass of 51 kg, which implies a resting vertical component around 250N (note that the force is divided by the two feet). Therefore, the vertical components induced by specific muscular activity to achieve this motion have to take that into account. Given this, the max peak values (in absolute table) are presented in table 3.1. An important aspect of our analysis is also that the plate 2 values are equal to 0 N across all the experimental procedures, since the jump was carried out from the first to the third plate.

Table 3.1: Max peak values (in absolute value) obtained for the vertical and horizontal components of GRFs. The results marked with "*" were obtained by discounting the gravitational weight of the subject. The normalized columns were obtained by dividing the Non-normalized value by the subject's weight (51kg).

	$\mathbf{F}_x$		$\mathbf{F}_z$	
	Non-Normalized (N)	Normalized (N/kg)	Non-normalized (N)	Normalized (N/kg)
Plate 1	134.26	2.63	459.19 (209.04*)	9.00
Plate 3	181.27	3.55	646.40 (396.15*)	12.67

From the entries marked with "*" it is now possible to confirm that the additional force applied by the muscles in the vertical component is not as distinct as the one applied on the horizontal axis, fact that is concordant with the what was mentioned in the previous part of this project: the horizontal component of the standing long jump has as much importance as the vertical one,[2] leading to the conclusion that both components have to be taken into consideration for a good performance. The fact that we could not find sufficiently consistent references to compare these values for this precise exercise hinders further conclusions at this level. Nevertheless, the discounted and normalized variables were here calculated as they might be more useful for consultation on this form.

From a temporal evolution point of view, it is possible observe that for both plots (horizontal and vertical component), there is an initial stage where there is only GRFs for the first plate. This stage consists of the countermovement and push-off phases and usually extends from 0% to around 70% of the cycle (in our case, to 58.371% approximately, being slightly early to the standard one. This should be taken into account in subsequent analyzes).[7] Then, there is a phase where no GRFs are detectable, as it refers to the flight phase and, finally, there is a last stage where GRFs are only detected in plate 3 - the landing phase, which in our case starts around 72.851% of the motion. An important point here is the fact that the horizontal component of the GRF in the landing phase is negative, as the applied force by the subject is leading to the breaking of the her motion.

Another interesting point is that the magnitude as of the horizontal as of the vertical components are both higher on the landing phase than in the propulsion phase. This fact can be assigned to the lack of technique/experience of our subject on this movement as almost no suspension was observed on the landing. In fact, the time on the initial stage to prepare for the flight phase is way larger than the one to land, and so the force applied to fly is more dispersed on time, while the force applied to break the motion is more concentrated but with higher magnitude.

Joint Moment

Similarly to what was performed for the gait, for the SLJ the lower limbs perform the pivotal role as far as performance is concerned. Given this, only the joint moments and powers are usually analysed in literature and so will we proceed. Our results are presented on Fig. 3.5.

As it can be observed, the results are quite similar on the propulsion stage. The most questionable ones are regarding to the knee, but an attentive look might suggest the main features of the curve - an initial positive moment and then a second peak around 50 % of the motion. The differences obtained for the landing stage can be assigned to the the fact that in the consulted reference,[7] the external forces were only measured on the propulsion phase. This can explain why from that point on only very smooth variations are observed. In fact, it is clear that for a complete analysis, some strong moments have to emerge in the lower limbs' joints during the landing phase so that the subject can break its velocity in both horizontal and vertical components. A final remark is left regarding the unities obtained by *Maćkała et al.*[7] in this figures, since taking into account the numeric values obtained, they seem inappropriate.

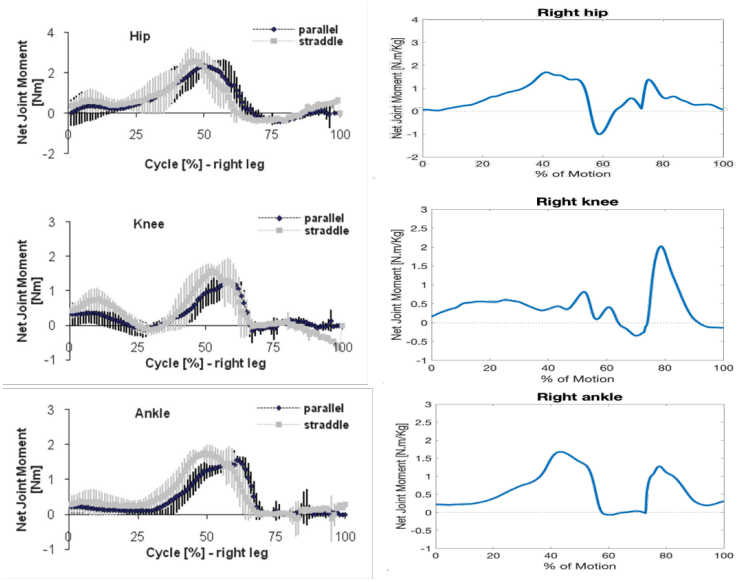

Figure 3.5: Moments obtained for the lower limbs' joints. The results described in the literature (*Maćkała et al.*[7]) are exposed on the left, whereas on the right, the ones obtained by the lab data can be found. On literature data, the curve to be taken into account is the "parallel" labelled curve, as it stands for the intial position of the feet in the propulsion stage.

Joint Power

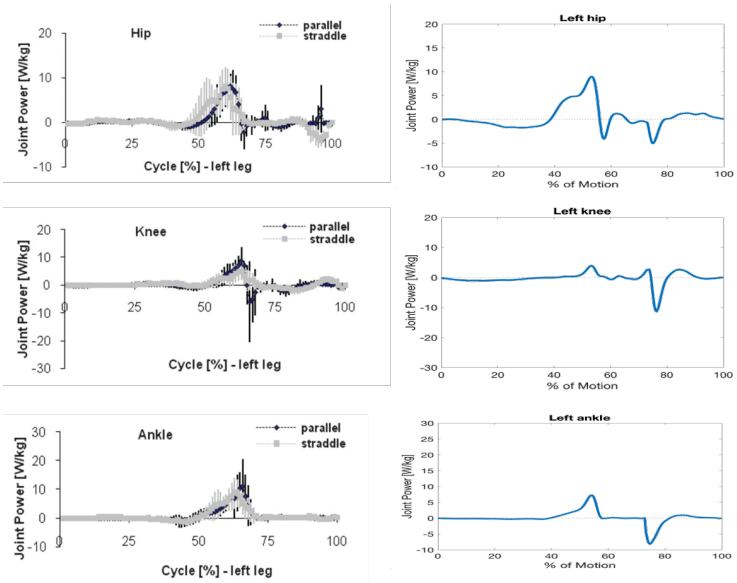

Figure 3.6: Powers obtained for the lower limbs' joints. The results described in the literature (*Maćkała et al.*[7]) are exposed on the left, whereas on the right, the ones obtained by the lab data can be found. Again, on the literature data, the curve to be considered is the "parallel" labelled curve

For the powers motion the same observation can be made as for the joint moments: the results between our implementation and the one on the literature are concordant, but from the landing phase on they diverge. A possible reason for this fact was already exposed in the previous section.

It should be pointed out that, by the way the powers are calculated from the joint moments, the unities considered in our work are now consistent with the ones provided by *Maćkała et al.*,[7] reinforcing our previous remark.

A last note is directed to the signal of the powers obtained: while for the propulsion phases, all the contractions are concentric - the power is positive since the muscles are generating moment in the direction we want to move towards on - in the landing phase, they're eccentric - the power is negative as our subject's muscles are generating moment in the opposite direction of the one that her joints are bending, leading to the stoppage of the motion.

3.3 Electromyography

Gait

The results were obtained in this section resorting to the root mean square (RMS) technique, even though with an unknown time window, of the raw EMG data. The results obtained are depicted in Fig. 3.7.

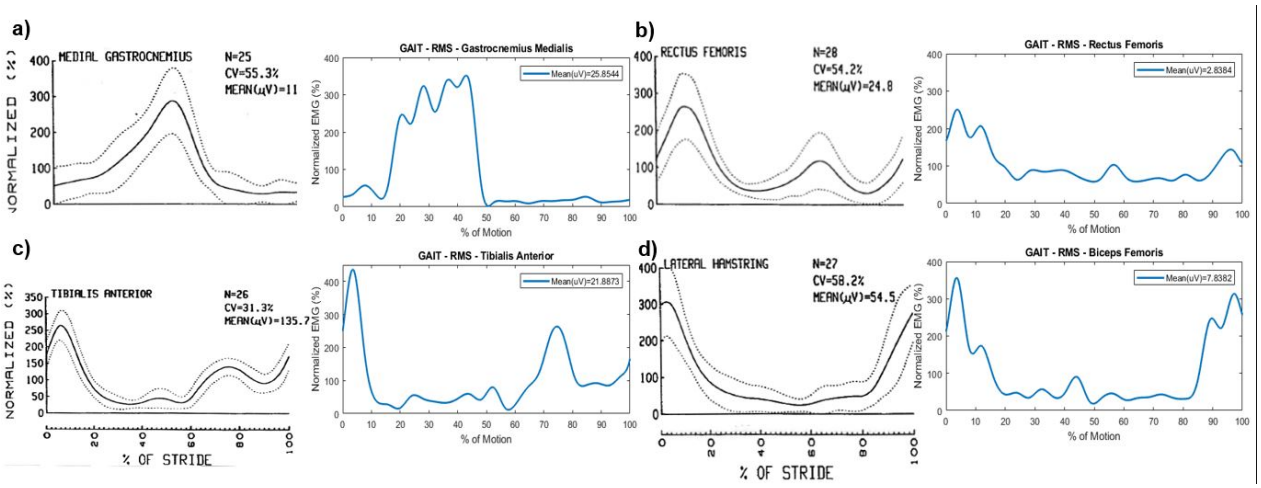

Figure 3.7: EMG for 4 different muscles - a) *Gastrocnemius Medialis*, b) *Rectus Femoris*, c) *Tibialis Anterior* and d) *Biceps Femoris* - in gait. For each muscle, the results depicted in literature (*Winter(1987)*)[4] (left) and retrieved from this lab data (right) are represented.

The authors[4] resorted to linear envelope (full wave rectification + low-pass filter) of the raw EMG to obtain their results. Therefore, as both techniques (RMS and linear envelope) are generally speaking rectifying and smoothing techniques, the procedures yield similar results (even though the RMS uses a non-causal filter). Nevertheless, it is important to mention that the relationship between the force of contraction and EMG activity is far from straightforward.[4] The normalization method used is both techniques was the same: normalization to the mean of the signal in μV as 100%.

Proceeding to the analysis of the data itself, in the *gastrocnemius medialis* (Fig. 3.7. a)) case , it is possible to observe that its maximal peak is consistent with literature, being associated to plantar flexion during the foot's lift off. The disturbance before it could be assigned to a hesitation of the subject, when trying to step on the force plates, as it happens right on the moment when the right heel starts to lift.[4]

Regarding the *Rectus Femoris* (Fig. 3.7. b)), its activation is required for weight acceptance, as this muscle acts as knee extensor. This can be observed in the EMG signal in the beginning of the gait, being related to the heel contact with the ground. Moreover, the spike around 55% of the cycle was expected to be larger and slightly deviated to the right, fact that might be assigned to the lower cadence of our subject's gait, as this spike would be requested for the hip flexion, pulling the thigh up, and knee extension, propelling the leg forward.[4]

As far as the *Tibialis Anterior* (Fig. 3.7. c)) is concerned, its major activation is observed to support the foot dorsiflexion at the end of the swing phase, proceeding to the stance as preparation for the contact of the foot with the ground. A second activation can be roughly seen in around 50% of the cycle, assigned to the toes lifting off, being responsible for foot clearance during mid swing. At last, there is one final peak pulling the leg forward at around 70% of the cycle.[4]

Finally, for *Biceps Femoralis* (Fig. 3.7. d)), the results obtained have slightly more oscillations than the one described in literature, which might be assigned to the fact that it was obtained from only one repetition. Nevertheless, the major peak occurs in the beginning and in the end of stride, when this muscle acts as hip extensor during weight acceptance and has a role in decelerating the leg, being consistent with what would be expected.[4]

Standing Long Jump

For the study of the SLJ, the RMS results was also used, as, this time, this was exactly the way used by the literature to process their data. Even though the time window used in *Maćkała et al.*[7] was known, our attempt of reproducing them from the EMG data was not successful, as smoothing step cut-off frequency information was missing. Therefore, for reasons of similarity, the data used was the one of unknown time window. Those results are exposed in Fig. 3.8.

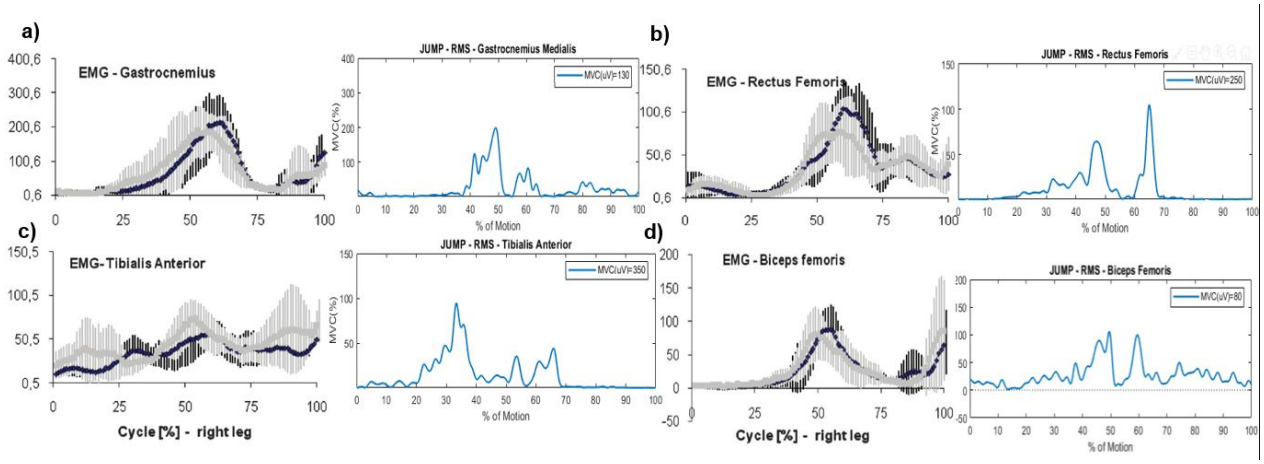

Figure 3.8: EMG for 4 different muscles - a) *Gastrocnemius Medialis*, b) *Rectus Femoris*, c) *Tibialis Anterior* and d) *Biceps Femoris* - in standing long jump. For each muscle, the results depicted in literature *Maćkała et al.*[7] (left) and the ones retrieved from this lab data (right) are represented.

Regarding the the normalization procedure, the literature resorted to percentage of the maximum voluntary contraction (MVC (%)). As we did not have access to the maximum voluntary contraction in our case, a value was arbitrarily chosen so that the values could be similar to the

ones in y-axis to the literature, as we're more interested in the comparison among shapes of those curves.

Generally speaking, the results obtained were not very similar to the ones described in literature, even though some similarities can be still observed. We assign these differences to the not clearly explained processing procedure.

Regarding the *gastrocnemius medialis* (Fig. 3.7. a)), it is possible to observe that it is mainly requested for the propulsion moment, playing an important role on the plantar flexion of the foot.

Rectus Femoris has two main activations: one for the propulsion phase, contributing to leg extension as a knee extensor and the other during the flight phase.

On the other hand, the *Tibialis Anterior* has its major activation peak in an initial stage of the propulsion, as it is required to maintain the equilibrium in the countermovement phase.

Finally, the *Biceps Femoris* shows a similar behaviour to the *Rectus Femoris*, even though the first activation emerges slightly after. This is due to the fact that these two muscles are antagonists and so, besides their important work in the propulsion force, an equilibrium is required in order to allow a good performance.

It is worth mentioning that both for *Rectus Femoris* as for *Tibialis Anterior* during the landing phase the signal is not typical (excessively near to 0), which might indicate that some disconnection might have happened due to the abrupt forces/acellerations in the initial part of this phase.

4 Conclusion

In this work, many relevant biomechanical variables could be analyzed not only in the gait context, but also in the standing long jump case. This type of study may not only play a pivotal role in the treatment of disorders but also in the improvement of many sports motion, through kinematic and dynamic optimization. As referred, the validation and precision of the methodology followed is verified, as these methods allow for the reproduction of results found in literature.

In fact, as for the gait as for the standing long jump, our dynamic analysis implementation revealed itself as a quite robust procedure, yielding results consistent with literature for both movements, at least as far as ground reaction forces and lower limbs' joint moments and powers are concerned.

For the EMG analysis, the results for the gait were consistent with the consulted literature, whereas the standing long jump implementation revealed itself not satisfactory, namely to the different filtration methods and cutoff frequencies that are used. Other factors involved in data acquisition may also play an important role, such as noise, humidity, and other physical conditions that affect the EMG acquisition.

Bibliography

[1] J. A. C. Ambrósio and A. Kecskeméthy, "Multibody Dynamics of Biomechanical Models for Human Motion via Optimization," pp. 245–272, 2007.

[2] A. Vieira, J. Evrard, M. Madeira, and M. Parreira, "Kinematic Analysis of Humam Movement: Gait and Standing Long Jump," tech. rep., Instituto Superior Técnico, Lisbon, 2019.

[3] M. Paz, *Structural Dynamics: Theory and Computation*. Springer US, 1991.

[4] D. Winter, *The biomechanics and Motor Control of Human Gait*. University of Waterloo Press, 1987.

[5] T. Andriacchi, J. Ogle, and J. Galante, "Walking speed as a basis for normal and abnormal gait measurements," *Journal of Biomechanics*, vol. 10, no. 4, pp. 261 – 268, 1977.

[6] J. Fang, A. Vuckovic, S. Galen, B. Conway, and K. Hunt, "Mechanical stimulation of the foot sole in a supine position for ground reaction force simulation," *Journal of neuroengineering and rehabilitation*, vol. 11, p. 159, 11 2014.

[7] M. Krzysztof, J. Stodółka, A. Siemieński, and M. Čoh, "Biomechanical analysis of standing long jump from varying starting positions," *Journal of strength and conditioning research / National Strength Conditioning Association*, vol. 27, 05 2012.

[8] D. A. WINTER, *Biomechanics and Motor Control of Human Movement*. 2009.

[9] I. S. T. Integrated Masters in Biomedical Engineering, "Biomechanics of Human Motion 2019-2020 - week 08," 2019.

[10] P. Flores, "Investigation on the baumgarte stabilization method for dynamic analysis of constrained multibody systems," 2008.

Appendix A

Preprocessing

The function *ReadProcessData()* projects the data into the sagittal plane: it takes the x and z coordinates for every point at each instant. Then the biomechanical model is built, formed of 15 points (P_1 to P_{15}) as it can be seen on Figure A.1. The function *FilteredCoordinates()* is called inside *ReadProcessData()* and with a low-pass filter treats the data.

The function *ComputeAverageLength()* is used to deal with small inconsistencies in lenght of bodies due to the projection step. The file *static.xlsx* provides static data (2 seconds) used for reference. At each time step and for each body, the length is calculated between the two edge points of the body and the average is computed.

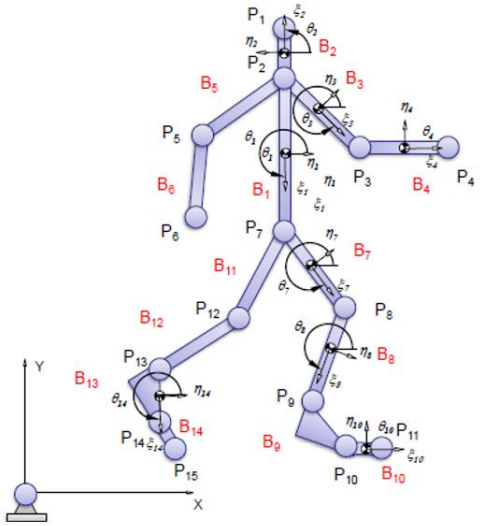

Figure A.1: Model with 14 bodies (from B1 to B14) and 15 points representing markers(from P1 to P15)

For the present project, only drivers of type I and III are implemented in function *EvaluateDrivers()*. Type I drivers describe the absolute coordinates of the multi-body system and refer to the trunk (body 1). Drivers of type III are defined as the difference of the orientation of two bodies, with angles defined with respect to the horizontal axis and measured counterclockwise: $\theta_{ij} = \theta_j - \theta_i$.

The function *FilteredCoordinates()* is based on the method that uses the residual analysis, described by *Winter (2009)*.[8] This method is a good compromise between reducing the noise present in the raw data while keeping the useful information. To determine which cut-off frequency f_c is the best, we process a residual analysis of the difference between filtered $\hat{X}_i$ and unfiltered X_i signals. This is computed over a wide range of cut-off frequencies (in the present case, 0.1Hz to 10Hz with a step of 0.1 Hz). For a gait cycle, the cut-off frequencies normally range between 2 and 6 Hz.[8]

Appendix B

Anthropometry

Table B.1: Mass, Center of Mass Location and Radius of Gyration: (50 Percentile - Adults - Male). Retrieved from Ambrósio (2019)[9]

Segment	Definition	Segment Weight/Total Body Weight	Center of Mass/ Segment Length		Radius of Gyration/ Segment Length		
			Proximal	Distal	C of G	Proximal	Distal
Hand	Wrist axis/knuckle II middle finger	0.006 M	0.506	0.494 P	0.297	0.587	0.577 M
Forearm	Elbow axis/ulnar styloid	0.016 M	0.430	0.570 P	0.303	0.526	0.647 M
Upper arm	Glenohumeral axis/elbow axis	0.028 M	0.436	0.564 P	0.322	0.542	0.645 M
Forearm and hand	Elbow axis/ulnar styloid	0.022 M	0.682	0.318 P	0.468	0.827	0.565 P
Total arm	Glenohumeral joint/ulnar styloid	0.050 M	0.530	0.470 P	0.368	0.645	0.596 P
Foot	Lateral malleolus/head metatarsal II	0.0145 M	0.50	0.50 P	0.475	0.690	0.690 P
Leg	Femoral condyles/medial malleolus	0.0465 M	0.433	0.567 P	0.302	0.528	0.643 M
Thigh	Greater trochanter/femoral condyles	0.100 M	0.433	0.567 P	0.323	0.540	0.653 M
Foot and leg	Femoral condyles/medial malleolus	0.061 M	0.606	0.394 P	0.416	0.735	0.572 P
Total leg	Greater trochanter/medial malleolus	0.161 M	0.447	0.553 P	0.326	0.560	0.650 P
Head and neck	C7–T1 and 1st rib/ear canal	0.081 M	1.000	— PC	0.495	0.116	— PC
Shoulder mass	Sternoclavicular joint/glenohumeral axis	—	0.712	0.288	—	—	—
Thorax	C7–T1/T12–L1 and diaphragm*	0.216 PC	0.82	0.18	—	—	—
Abdomen	T12–L1/L4–L5*	0.139 LC	0.44	0.56	—	—	—
Pelvis	L4–L5/greater trochanter*	0.142 LC	0.105	0.895	—	—	—
Thorax and abdomen	C7–T1/L4–L5*	0.355 LC	0.63	0.37	—	—	—
Abdomen and pelvis	T12–L1/greater trochanter*	0.281 PC	0.27	0.73	—	—	—
Trunk	Greater trochanter/glenohumeral joint*	0.497 M	0.50	0.50	—	—	—
Trunk head neck	Greater trochanter/glenohumeral joint*	0.578 MC	0.66	0.34 P	0.503	0.830	0.607 M
Head, arms, and trunk (HAT)	Greater trochanter/glenohumeral joint*	0.678 MC	0.626	0.374 PC	0.496	0.798	0.621 PC
HAT	Greater trochanter/mid rib	0.678	1.142	—	0.903	1.456	—

Appendix C

Cut off Frequencies

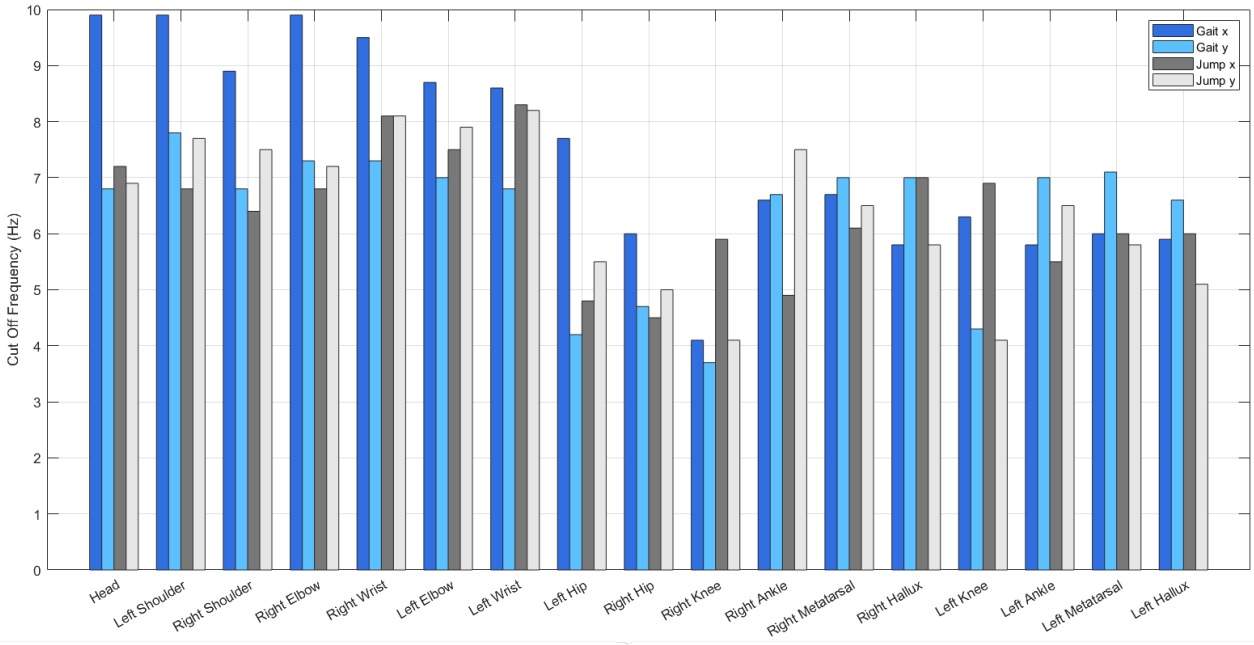

Figure C.1: Cut off frequencies used for filtration of the position data of each body, for both movements.

Appendix D

Details on processing method

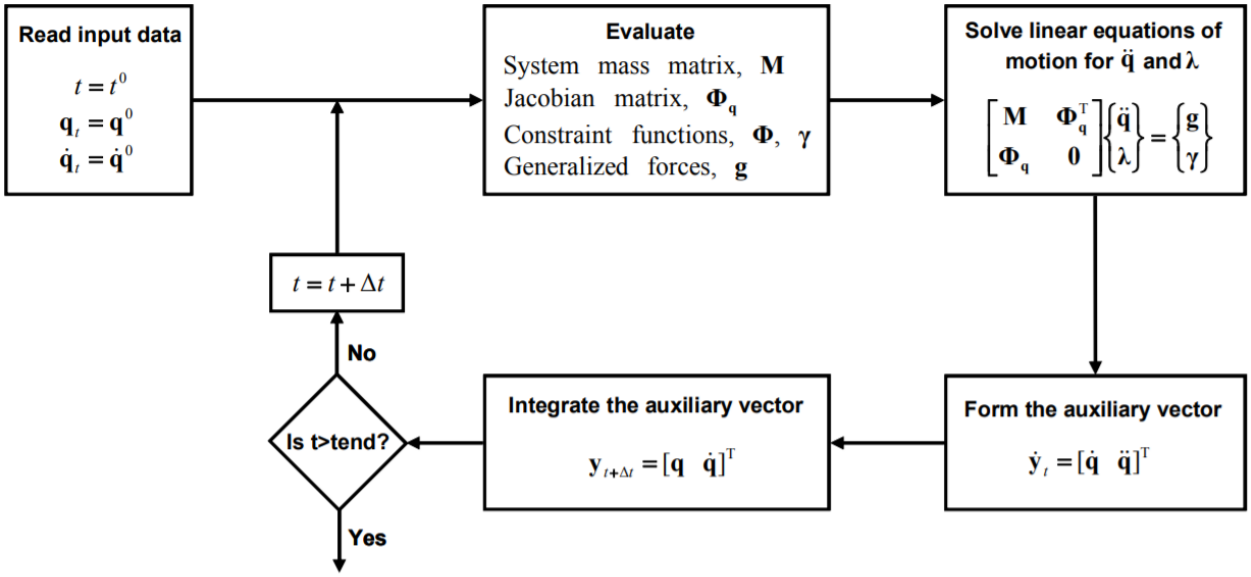

Figure D.1: Flowchart for the direct dynamic analysis. Retrieved from Ambrósio et al (2007)[1]

In the system, only the acceleration constraint equations are explicitly used, which leads to the propagation of small numerical errors. To fix this problem, the **Baumgarte stabilizer** is implemented. The principle of this method is to damp out the acceleration constraint violations by feeding back the violations of the position and velocity constraints.[10] Its main drawback is the correct selection of the feedback parameters α and β. In our case, they were given, both with a value of 5. The system now takes this form:

$$\begin{bmatrix} M & \Phi_q^T \\ \Phi_q & 0 \end{bmatrix} \begin{Bmatrix} \ddot{q} \\ \lambda \end{Bmatrix} = \begin{Bmatrix} g \\ \gamma - 2\alpha(\Phi_q \dot{q} - \nu) - \beta^2 \Phi \end{Bmatrix} \tag{D.1}$$

Mass matrix: The mass matrix M in equation D.1 is a diagonal matrix of individual mass matrices, M_i, of each body i. Each M_i is also a diagonal matrix given by equation D.2, where m_i and J_i are the body's mass and inertia, respectively. This structure is created inside the function *BuildMassMatrix()*.

$$M_i = \begin{bmatrix} m_i & 0 & 0 \\ 0 & m_i & 0 \\ 0 & 0 & J_i \end{bmatrix} \tag{D.2}$$

External forces: The vector of external force g includes the gravity forces and the contact forces. Assuming that we have n_b bodies: $g = [g_1, g_2, ..., g_{n_b}]^T$. For each body i, the force f and the moment n applied on it, is written in the vector g_i:

$$g_i = \begin{bmatrix} f_{i\_x} \\ f_{i\_y} \\ n_i + n_{i\_transport} \end{bmatrix} = g_{i\_gravity} + g_{i\_contact} \tag{D.3}$$

The moment is composed of two terms, n_i and $n_{transport}$ the moment resulting from the product of the force f_i and the distance s_i^P between the application point of this force and the body's center of mass. It can be expressed as: $n_{transport} = s_x^P f_x - s_y^P f_y$. The function that implements the external forces is called *BuildForceVector()*.